Supplementary information for

Ultrathin MXene Conductive Films with Percolation-Driven Electron Transport and Thickness-Dependent Microwave Absorption/Shielding Dual Functionality

Dong Wen, Xu Zhou, Qianqian Fan, Can Cui, Kan Fang, Ling Ding, Xiaoai Ye, Shihao Zheng, Zhaokun Jiang, Yanke Zhou, Daqiang Zhao, Gui-Gen Wang*

Guangdong Provincial Key Laboratory of Semiconductor Optoelectronic Materials and Intelligent Photonic Systems, School of Materials Science and Engineering, Harbin Institute of Technology (Shenzhen), Shenzhen, 518055 P. R. China

Corresponding Author: wangguigen@hit.edu.cn

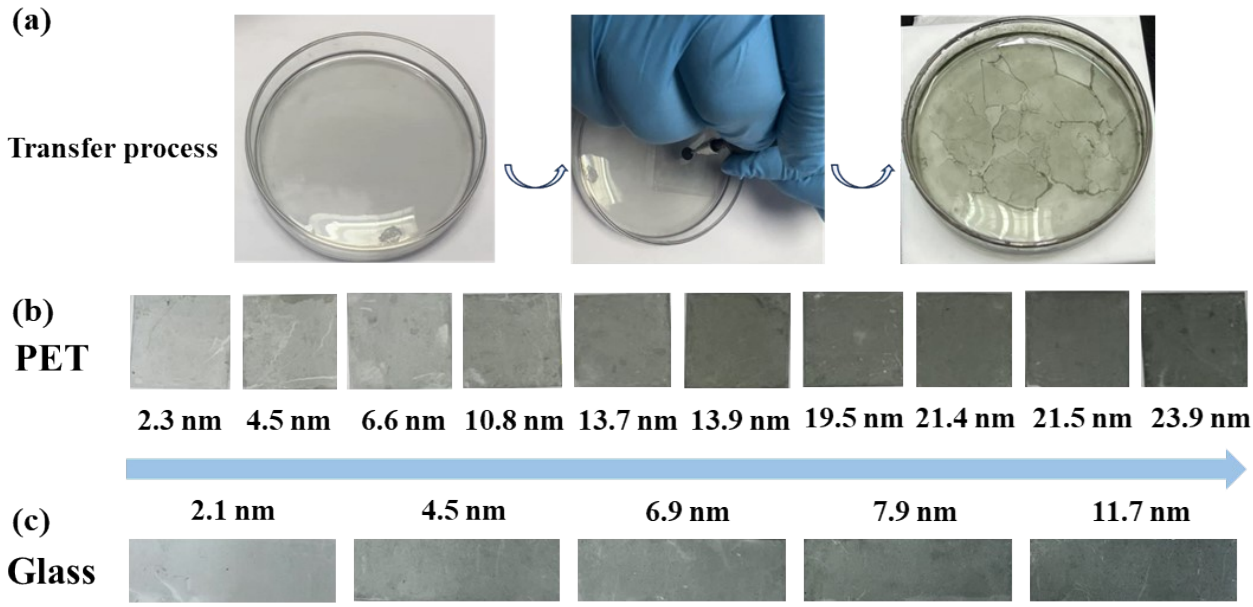

Figure S1 (a) Transfer process and Digital images of ultrathin $Ti_3C_2T_x$ films with different thicknesses transferred onto (b) PET and (c) Glass substate.

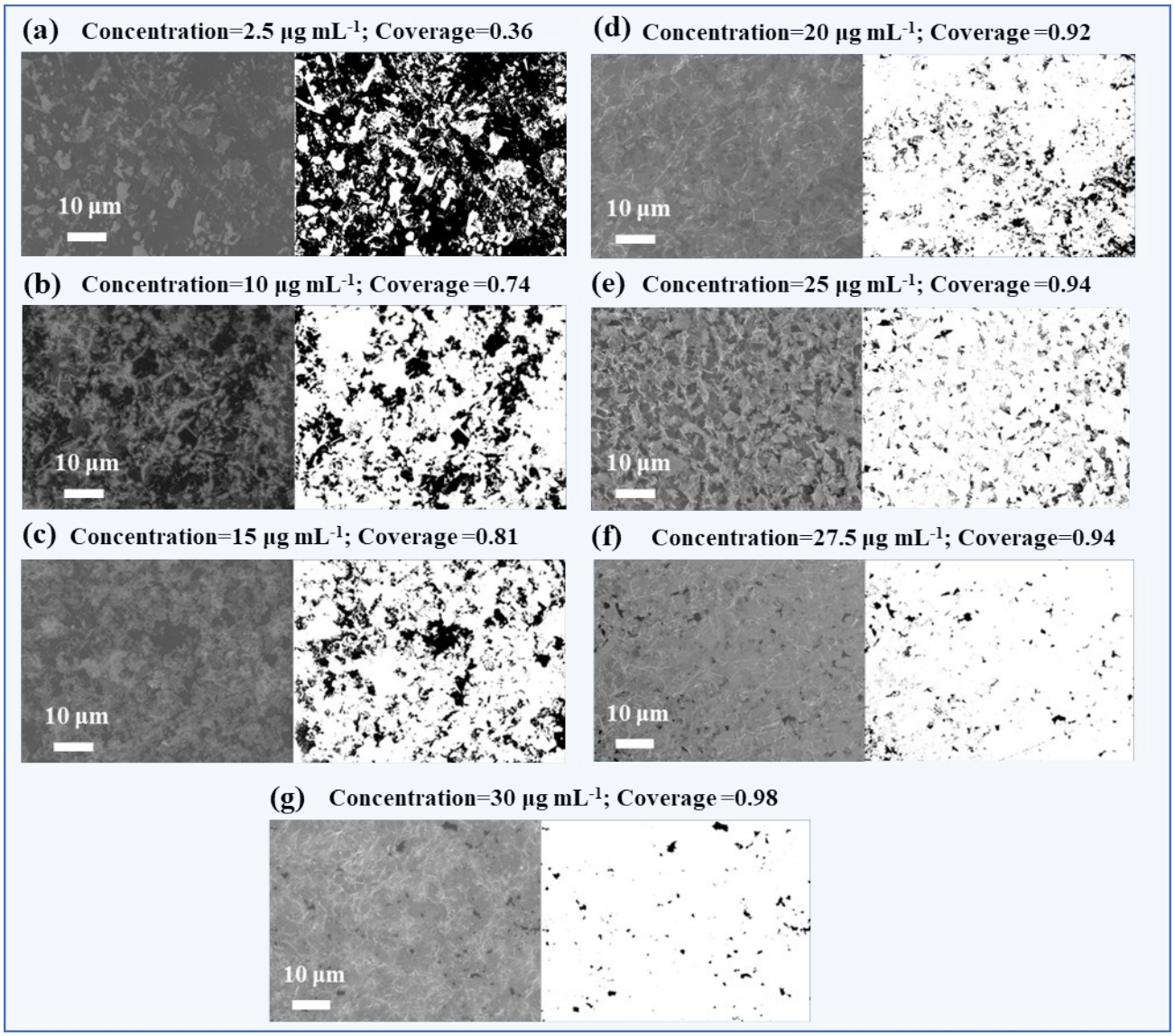

Figure S2 Morphology characterization of monolayer $Ti_3C_2T_x$ films. (a-e) Left: SEM image of transferred monolayer $Ti_3C_2T_x$ films with different coverage on PET substrate: Right: Analyzed image using ImageJ software showing the coverage of substrate by the $Ti_3C_2T_x$ nanosheets. All scale bars = 10 μm, and black areas represent uncovered areas in all bottom images.

Nanosheet coverage (c) was defined as the fractional area occupied by $Ti_3C_2T_x$ MXene nanosheets, including overlapping regions, relative to the total substrate area. The coverage c was then calculated from the ratio of white pixels ($Ti_3C_2T_x$ nanosheets) to total pixels in binarized SEM images.

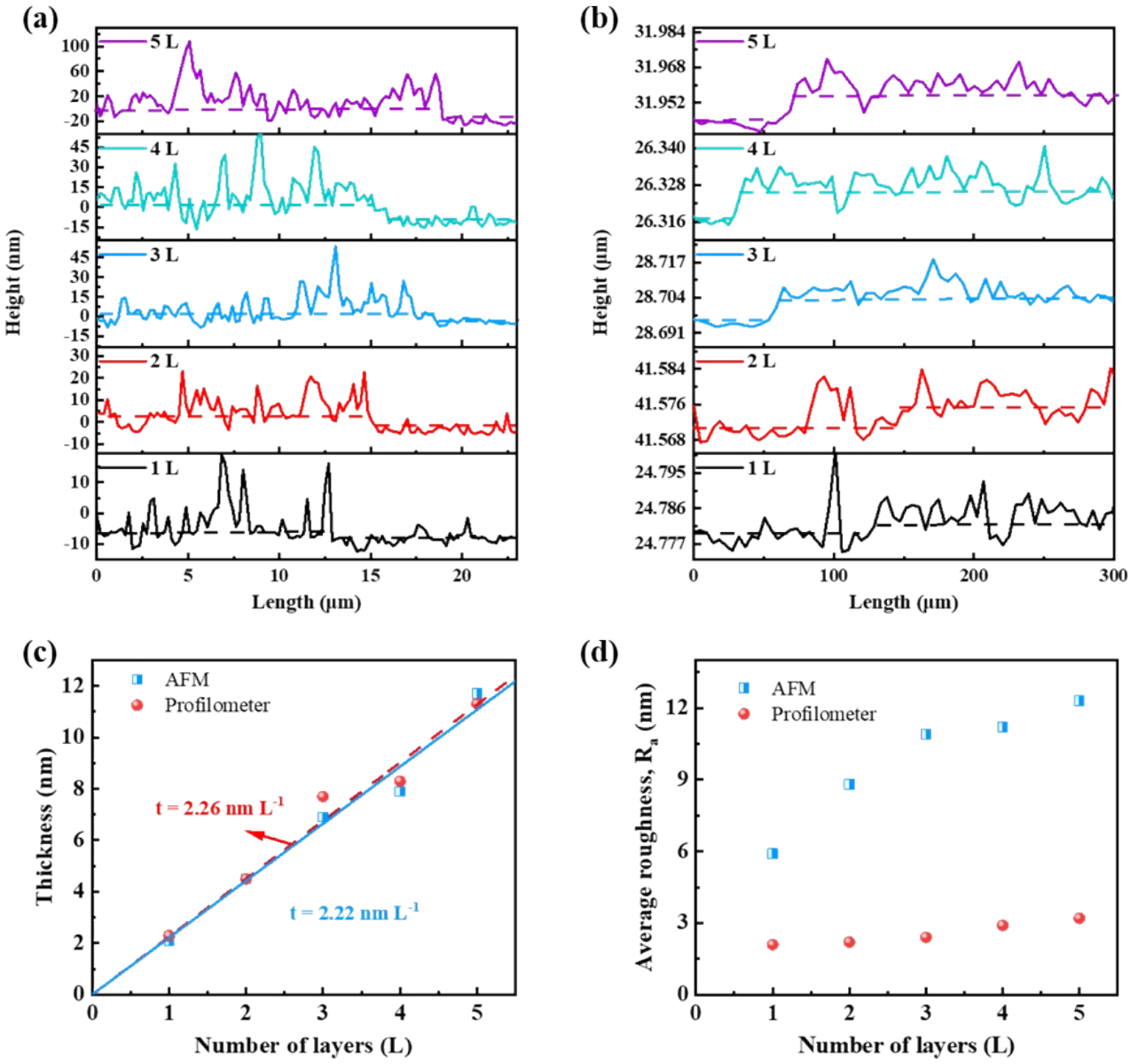

Figure S3 (a) AFM height profiles and (b) profilometer height profiles of transferred 1~5 L $Ti_3C_2T_x$ films. (c) Thickness and (d)average roughness for various layer stacking numbers of $Ti_3C_2T_x$ films

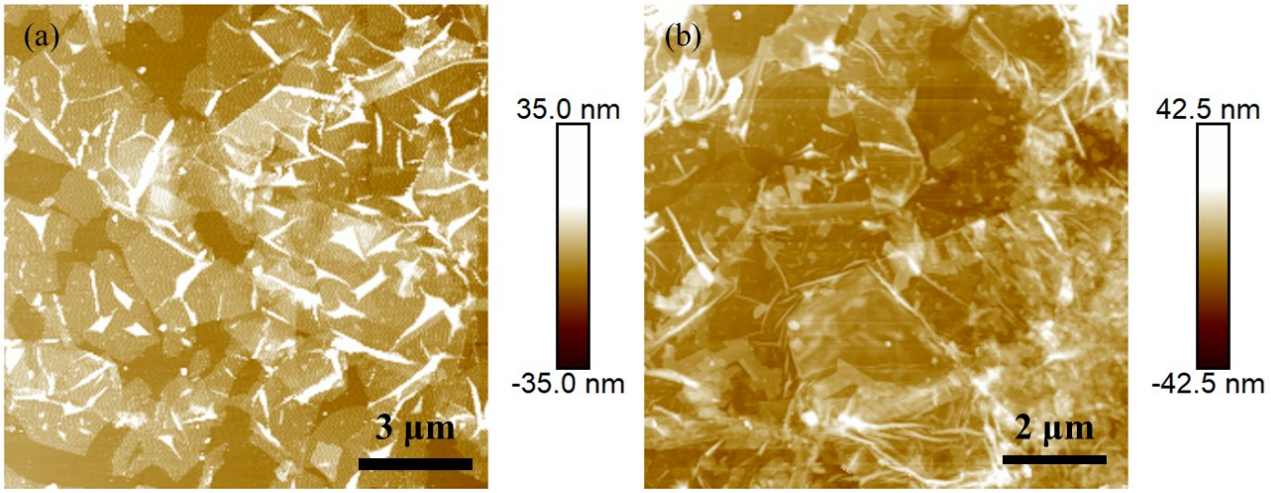

Figure S4 (a-b) Surface topography of monolayer $Ti_3C_2T_x$ films were measured by AFM in different regions.

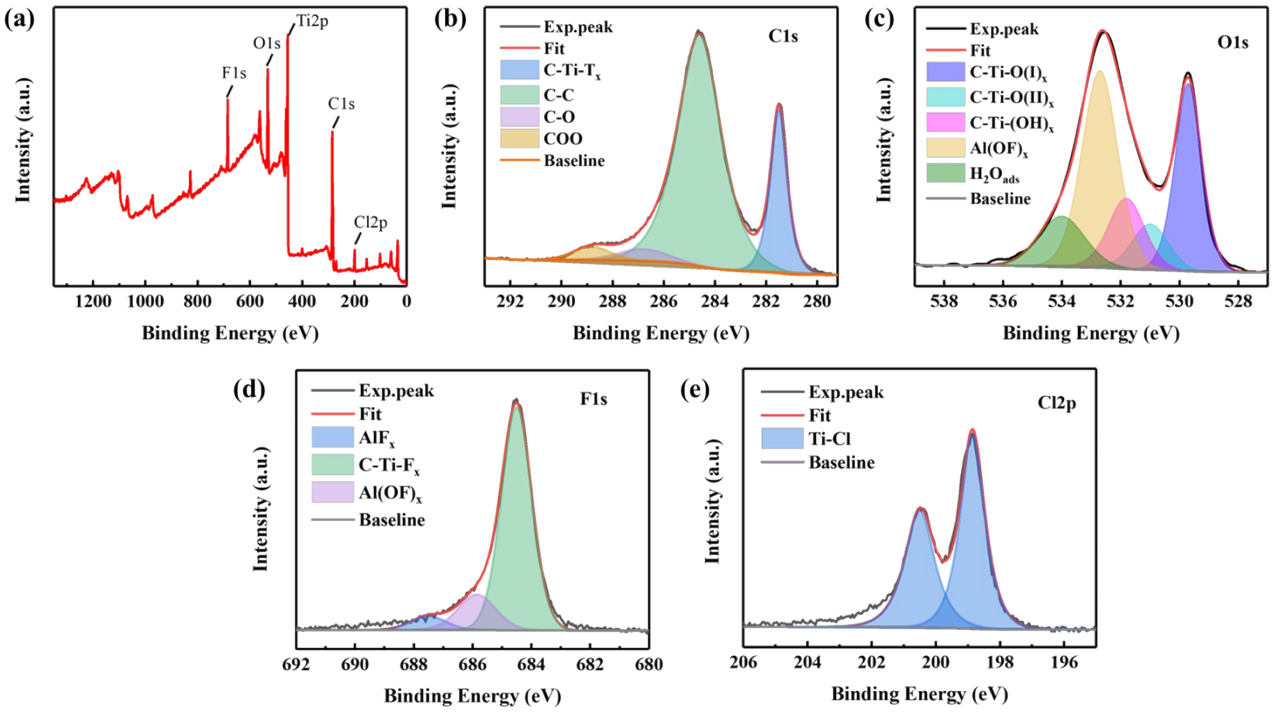

Figure S5 (a) XPS survey spectrum. (b) C1s, (c) O1s, (d) F1s, and (e) Cl2p XPS spectra of the $Ti_3C_2T_x$ film.

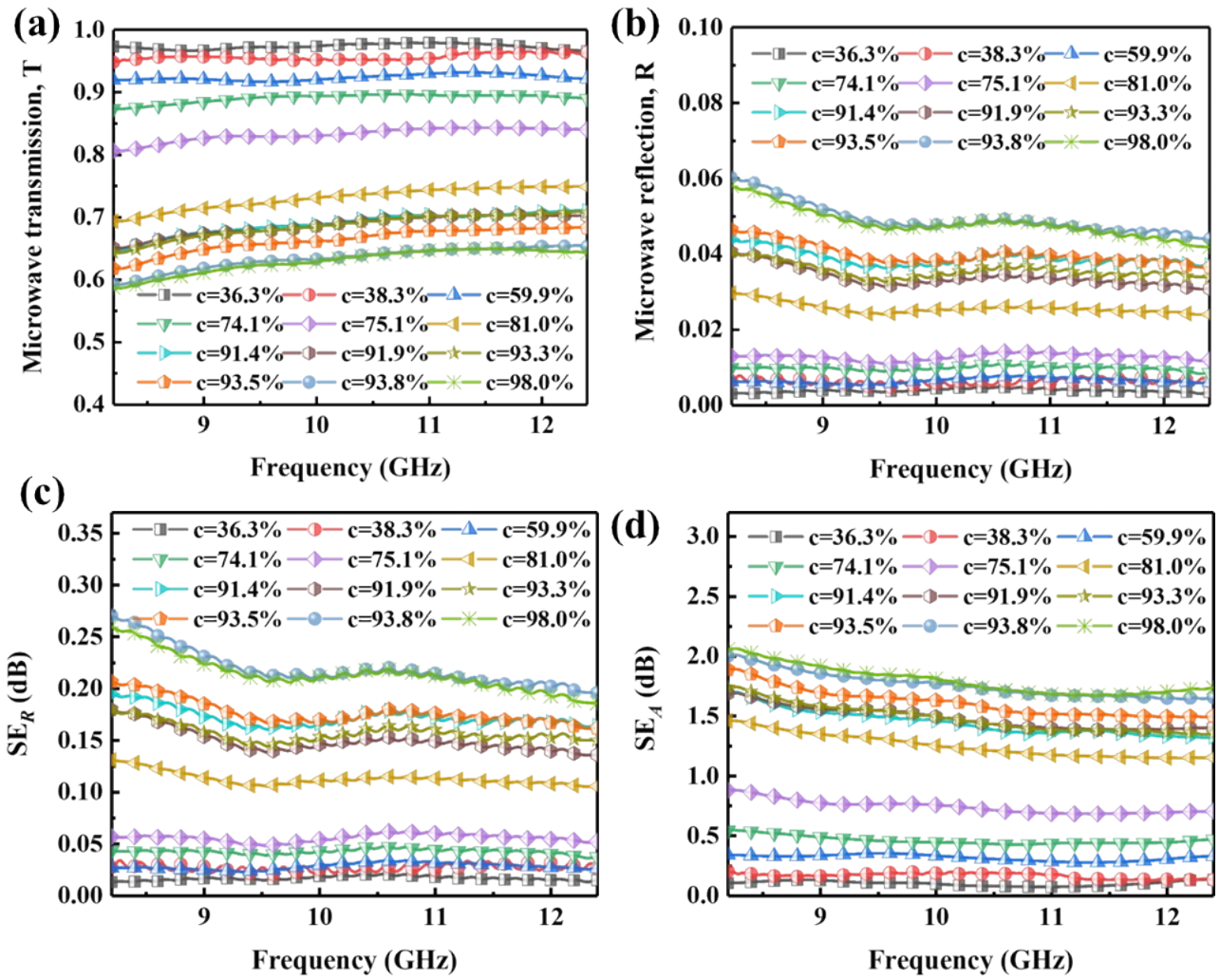

Figure S6 (a) Microwave tansmission T, (b) Microwave reflection R, (c) SE$_R$ values and (d) SE$_A$ values of monolayer $Ti_3C_2T_x$ films with different coverage in X-band.

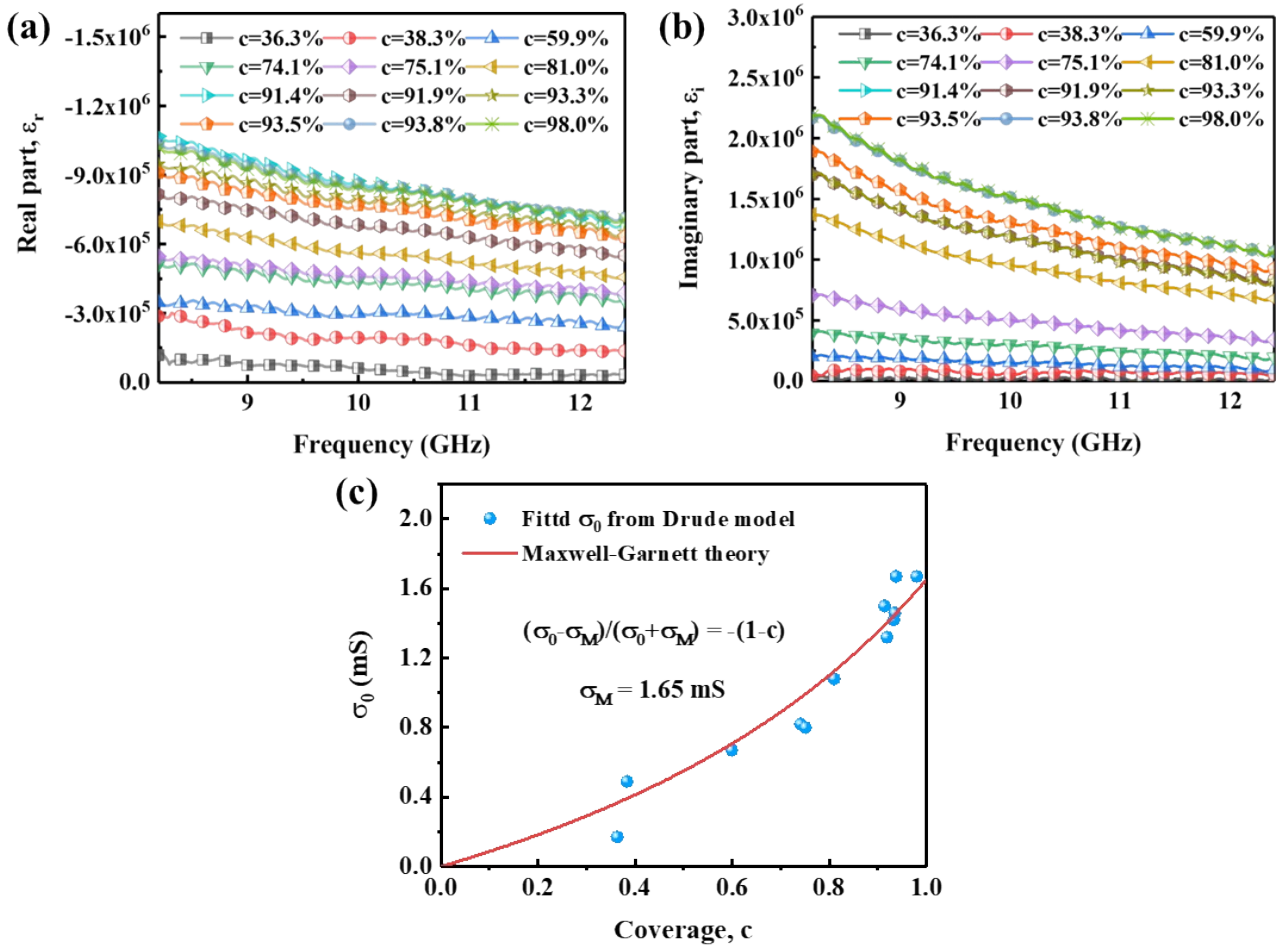

Figure S7 (a-b) The relative permittivity and (c) fitted sheet DC conductivity (σ_0) parameters of monolayer $Ti_3C_2T_x$ film with different coverage.

Table S1 Comparison of optoelectronic properties in submicron-thick $Ti_3C_2T_x$ MXene films

$Ti_3C_2T_x$ film	Thickness (nm)	Roughness (nm)	Optical conductivity (S cm^{-1})	Electrical conductivity (S cm^{-1})	FoM	Refs.
Slot-Die Coating	300	10.3	675	13000	18.5	1
Slot-Die Coating	350	12.6	675	7425	11	1
Inkjet Printing	187	18	320	41.6	0.13	2
Spray coating	40	12	-	13000	-	3
Spray coating	70	10	574	402	0.7	4
Gravure printing	70	15	680	4000	5.9	5
Dip-Coating	30	2.5	425	6375	15	6
Spin coating	81	8.7	890	6500	7.3	7
Interfacial self-assembly	24	12	1310	13000	10	This work

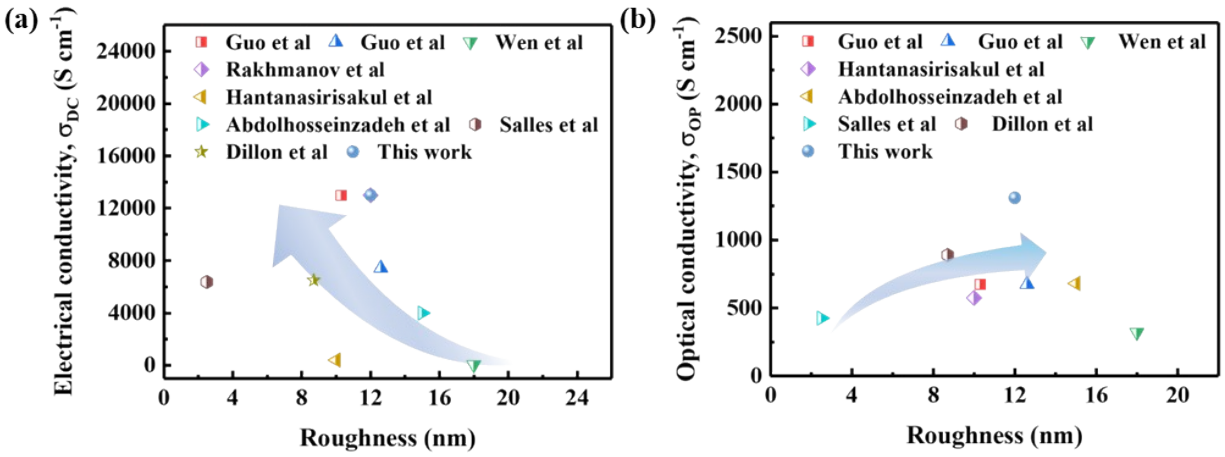

Figure S8 (a-b) Influence of roughness on electronic and optical conductivity in submicron-thick $Ti_3C_2T_x$ MXene films.

Table S2 Comparison of optoelectronic properties in sub-10 nm-thick $Ti_3C_2T_x$ MXene films

$Ti_3C_2T_x$ film	Flakes size (μm)	Thickness (nm)	Roughness (nm)	Optical conductivity (S cm^{-1})	Electrical conductivity (S cm^{-1})	FoM	Refs.
Interface self-assembly	10	3	1.8	-	285		[8]
Interfacial self-assembly	5	2.3	3	1248	2898	2.3	[9]
Spin coating	3.2	4	2	520	5736	11.03	[10]
Spin coating	-	2.5	2.6	890	4000	4.5	[7]
Spray coating	-	4	2	-	10000		[3]
Spray coating	0.5	5	5	574	250	0.43	[4]
Blade coating	12.2	2.5	1	750	9780	11.7	[11]
Slot-die coating	6	2.2	0.93	675	8906	13.2	[1]
Liquid-Liquid interface self-assembly	5	1.8	1.7	1254	555	0.44	[12]
Liquid-Liquid interface self-assembly	5	2	1	435	3081	7.8	[13]
Dip-Coating	1.4	7.2	2.5	314	1348	4.29	[6]
Gravure printing	-	1.9	5	680	1760	2.59	[5]
Interfacial self-assembly	11	2.3	5.7	1310	2717	2.07	This work

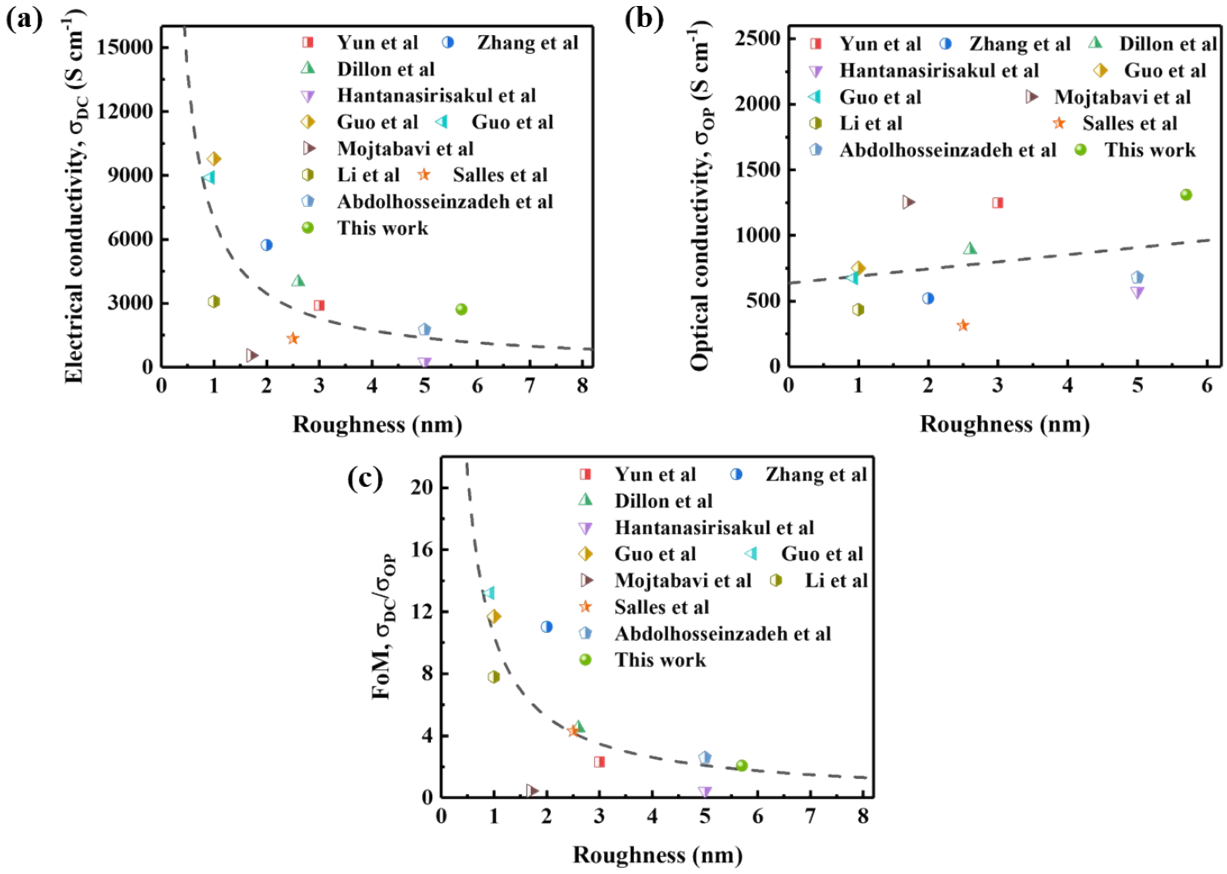

Figure S9 (a-c) Influence of roughness on electronic conductivity, optical conductivity and FoM in sub-10 nm-thick $Ti_3C_2T_x$ MXene films.

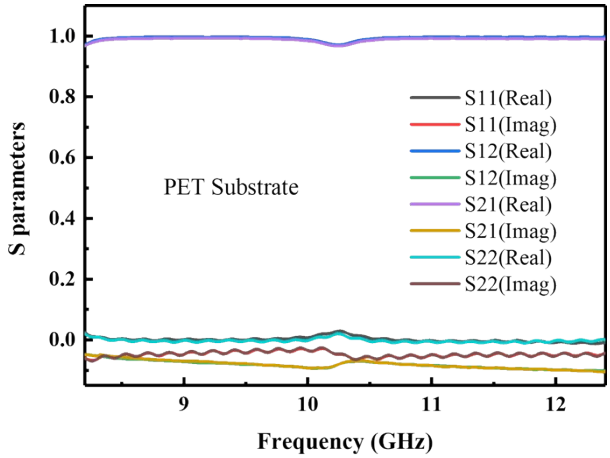

Figure S10 The S-parameters of the PET substrate in X-band.

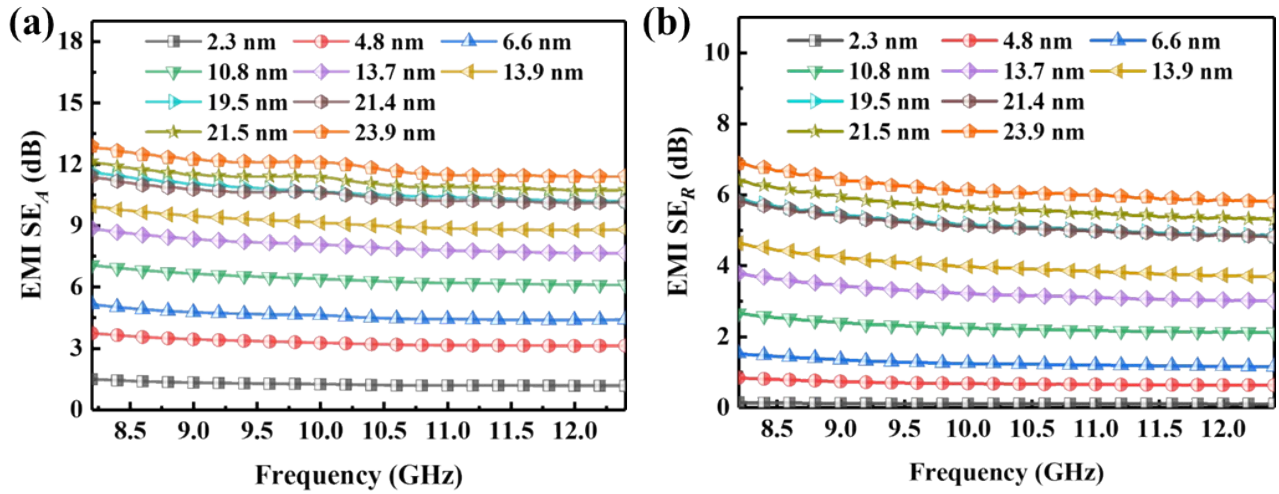

Figure S11 (a) SE_A values and (b) SE_R values of continuous $Ti_3C_2T_x$ films with different thicknesses in X-band.

Table S3 Comparison of absolute shielding effectiveness of various shielding materials

Film Samples	Thickness (cm)	SEt (dB)	SE_A (dB)	SE_R (dB)	SSE/t (dB cm^2 g^{-1})	Absorption (A)	Refs.
rGO/ Fe_3O_4	0.03	24	15	8	1.0×10^3	0.155	14
Graphene /CNTs	0.16	36	31	4	2.3×10^3	0.398	15
Graphene /CNWs	0.16	38	27	11	4.0×10^4	0.079	16
Graphene	8.4×10^{-4}	20	7	13	1.3×10^4	0.040	17
Graphene	0.005	60	-	-	1.8×10^4	-	18
Graphene	0.001	52	34	18	7.8×10^3	0.016	19
Ag nanofiber	0.0001	20	1.4	18.6	1.0×10^6	0.004	20
Silver	2×10^{-5}	51	12	39	2.4×10^5	0.0001	21
AgNWs	6.4×10^{-6}	20.4	14	6.5	3.0×10^5	0.215	22
	1.2×10^{-5}	13.5	10	3.5	1.1×10^5	0.402	
Al Foil	0.0008	66	-	-	3.1×10^4	-	23
Al	2×10^{-5}	24	-	-	4.4×10^5	-	24
Cu Foil	0.001	70	-	-	7.8×10^3	-	23
Cu mesh	0.00025	40.4	28.4	12	1.8×10^4	0.063	25
Copper	0.31	90	-	-	32	-	26
CuNi	0.15	25	2.5	22.5	690	0.0025	27
Ni mesh	0.0006	40	-	-	1.8×10^5	-	28
AgNi meshi	0.0004	43	-	-	2.9×10^5	-	29
AgNWs/Ni mesh	0.0003	41.5	-	-	3.7×10^5	-	30
Ti_3CNT_x	0.1	42.3	32.3	10	3.8×10^4	0.10	31

Ti_3CNT_x	0.001	43.5	-	-	4.0×10^6	-	32
	0.002	47.9	-	-	2.2×10^6	-	
	0.003	53.3	-	-	1.6×10^6	-	
	0.004	61.4	-	-	1.4×10^6	-	
$Ti_3C_2T_x$	2.3×10^{-7}	1.03	1	0.03	1.9×10^6	0.20	9
	6.9×10^{-7}	6.42	5	1.42	3.9×10^6	0.49	
	1.15×10^{-6}	9.31	6.8	2.5	3.4×10^6	0.45	
	1.61×10^{-6}	11.89	8	4	3.1×10^6	0.33	
	2.07×10^{-6}	13.84	9.5	4.5	2.8×10^6	0.31	
	3.45×10^{-6}	14.78	10	4.8	1.8×10^6	0.30	
	4.14×10^{-6}	17.13	11	6	1.7×10^6	0.23	
$Ti_3C_2T_x$	1.4×10^{-7}	1.4	1.2	0.2	4.2×10^6	0.23	33
	0.0014	70	-	-	2.1×10^4	-	
$Ti_3C_2T_x$	0.0001	48.4	-	-	1×10^5	-	34
	0.00011	26	17	9	9.9×10^4	0.12	35
	0.00025	57.4	37.4	20	7.8×10^4	0.01	36
	0.00028	60.8	-	-	7.2×10^4	-	37
	0.00031	61.3	41.3	22	6.2×10^4	0.006	38
	9.4×10^{-5}	50	46	14	1.2×10^5	0.040	39
	0.0007	58.4	43.5	15	3.5×10^4	0.032	40
$Ti_3C_2T_x$	4×10^{-7}	7	6.5	1.6	7.3×10^6	0.49	3
	15×10^{-7}	10	7	3	2.8×10^6	0.40	
	25×10^{-7}	19	12.5	6.5	3.2×10^6	0.21	
	40×10^{-7}	22	8	14	2.3×10^6	0.034	
$Ti_3C_2T_x$	2.3×10^{-7}	1.60	1.49	0.11	2.9×10^6	0.28	This work
	4.8×10^{-7}	3.97	3.28	0.69	3.5×10^6	0.45	
	6.6×10^{-7}	5.84	4.58	1.26	3.7×10^6	0.48	
	10.8×10^{-7}	8.66	6.39	2.27	3.4×10^6	0.46	
	13.7×10^{-7}	11.27	8.03	3.24	3.4×10^6	0.40	
	13.9×10^{-7}	13.12	9.13	3.99	3.9×10^6	0.35	
	19.5×10^{-7}	15.83	10.65	5.18	3.4×10^6	0.28	
	21.4×10^{-7}	15.63	10.49	5.14	3.1×10^6	0.28	
	21.5×10^{-7}	16.84	11.18	5.66	3.3×10^6	0.25	
	23.9×10^{-7}	19	12.85	6.15	3.3×10^6	0.23	

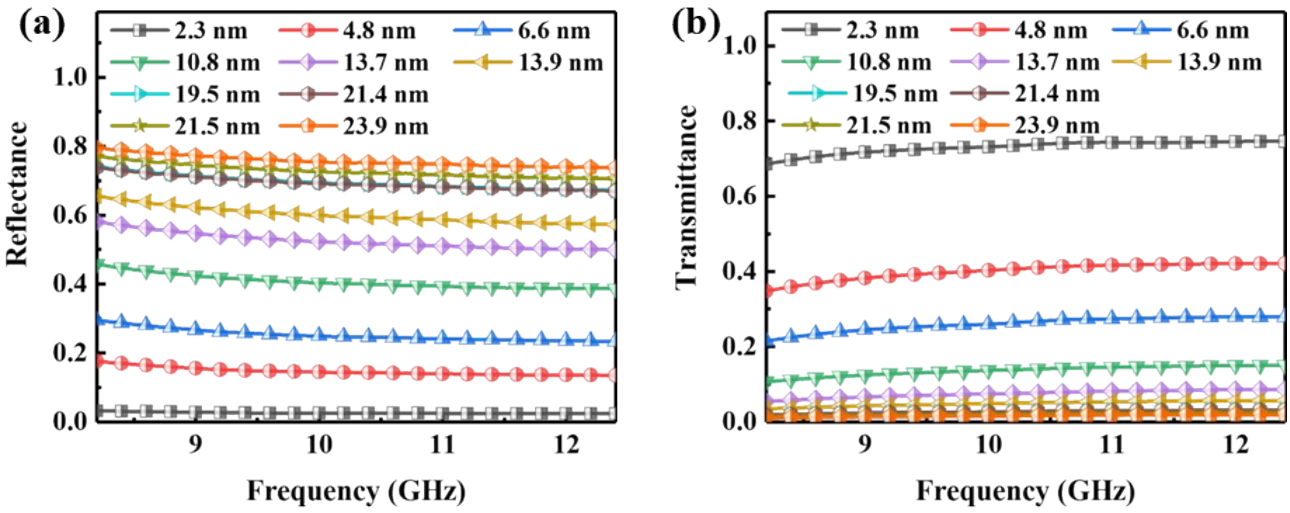

Figure S12 (a) Microwave reflection R, (b) Microwave tansmission T of continuous $Ti_3C_2T_x$ films with different thicknesses in X-band.

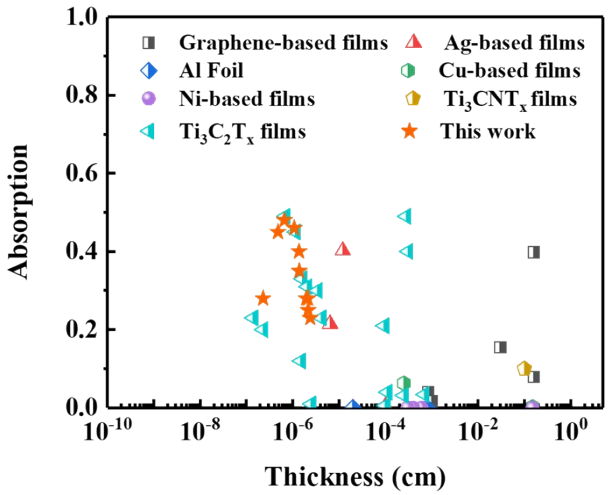

Figure S13 Performance comparison of different materials toward microwave absorption films.

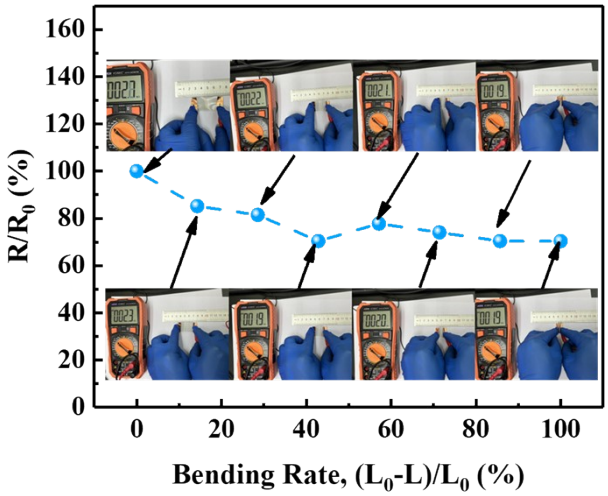

Figure S14 Bending test of a MXene film on a flexible PET substrate

18

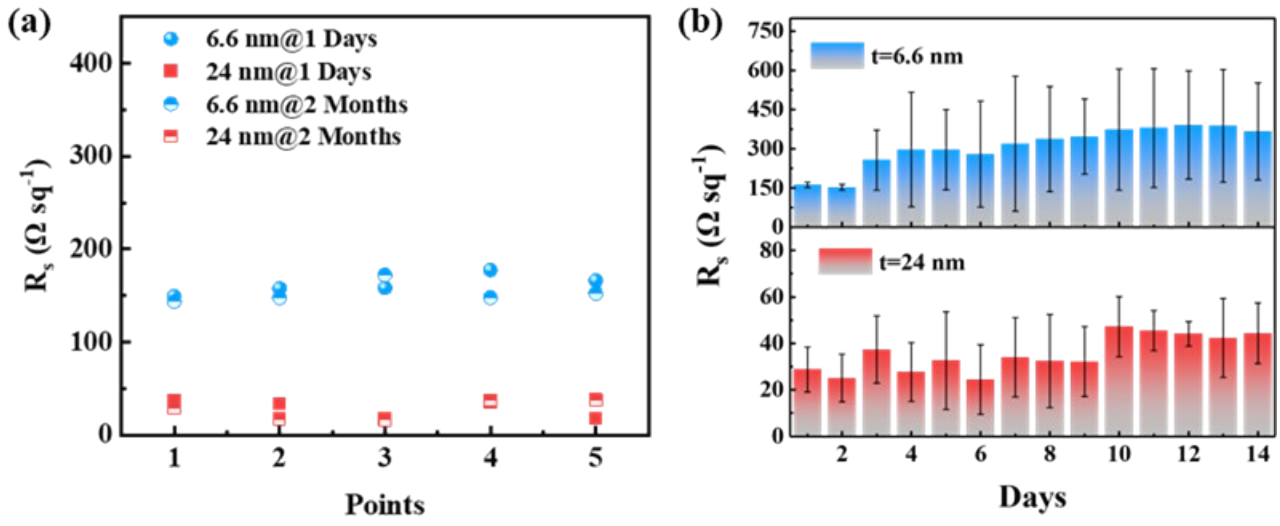

Figure S15 Stability test of electrical properties for MXene films under different storage conditions. (a) MXene films stored under vacuum conditions for 2 months; (b) MXene films placed in indoor natural environment.

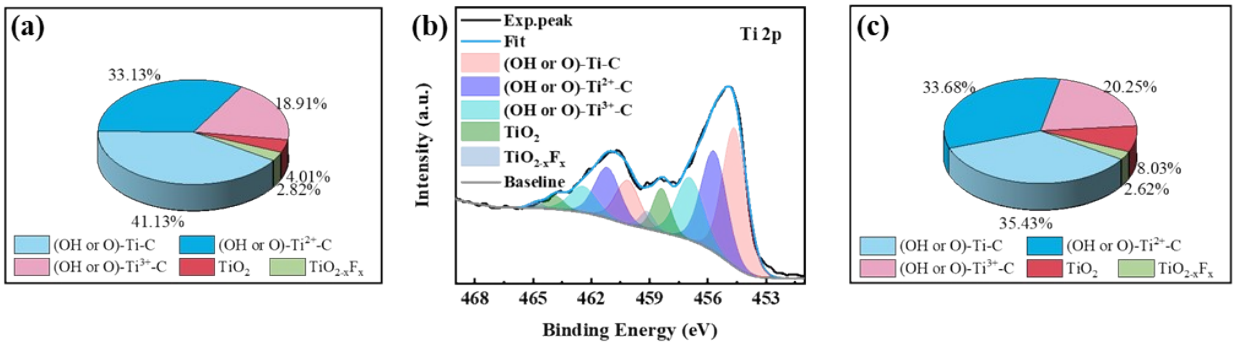

Figure S16 Elemental composition analysis. (a) Elemental composition of as-prepared MXene films; (b) High-resolution Ti 2p XPS spectra and (c) elemental composition of MXene films after being placed in indoor natural environment for 2 weeks.

Table S4 XPS peak fitting results for $Ti_3C_2T_x$ MXene films

Samples	Ti 2p	BE (eV)	FWHM(eV)	At. %	Refs.
As-prepared	(OH or O)-Ti-C	454.6(460.44)	1.3	41.13	2
	(OH or O)-Ti^{2+}-C	455.65(461.45)	1.44	33.13	
	(OH or O)-Ti^{3+}-C	456.9(462.45)	1.54	18.91	
	TiO_2	458.4(463.95)	1.11	4.01	
	$TiO_{2-x}F_x$	459.2(465.25)	1.15	2.82	
After 2 weeks	(OH or O)-Ti-C	454.6(460.1)	1.44	35.43	2
	(OH or O)-Ti^{2+}-C	455.65(461.15)	1.54	33.68	
	(OH or O)-Ti^{3+}-C	456.9(462.4)	1.63	20.25	
	TiO_2	458.35(463.85)	1.06	8.03	
	$TiO_{2-x}F_x$	459.1(464.84)	0.87	2.62	

References

1. T. Guo, D. Zhou, M. Gao, S. Deng, M. Jafarpour, J. Avaro, A. Neels, E. Hack, J. Wang, J. Heier and C. Zhang, *Adv. Funct. Mater.*, 2023, **33**, 2213183.
2. D. Wen, X. Wang, L. Liu, C. Hu, C. Sun, Y. Wu, Y. Zhao, J. Zhang, X. Liu and G. Ying, *ACS Appl. Mater. Interfaces*, 2021, **13**, 17766–17780.
3. R. Rakhmanov, C. E. Shuck, J. Al Hourani, S. Ippolito, Y. Gogotsi and G. Friedman, *Appl. Phys. Lett.*, 2023, **123**.
4. K. Hantanasirisakul, M. Q. Zhao, P. Urbankowski, J. Halim, B. Anasori, S. Kota, C. E. Ren, M. W. Barsoum and Y. Gogotsi, *Adv. Electron. Mater.*, 2016, **2**, 1600050.
5. S. Abdolhosseinzadeh, R. Schneider, M. Jafarpour, C. Merlet, F. Nüesch, C. Zhang and J. Heier, *Adv. Electron. Mater.*, 2025, **11**, 2400170.
6. P. Salles, D. Pinto, K. Hantanasirisakul, K. Maleski, C. E. Shuck and Y. Gogotsi, *Adv. Funct. Mater.*, 2019, **29**, 1809223.
7. A. D. Dillon, M. J. Ghidiu, A. L. Krick, J. Griggs, S. J. May, Y. Gogotsi, M. W. Barsoum and A. T. Fafarman, *Adv. Funct. Mater.*, 2016, **26**, 4162-4168.
8. T. Zhao, P. Xie, H. Wan, T. Ding, M. Liu, J. Xie, E. Li, X. Chen, T. Wang and Q. Zhang, *Nat. Photonics*, 2023, **17**, 622-628.
9. T. Yun, H. Kim, A. Iqbal, Y. S. Cho, G. S. Lee, M.-K. Kim, S. J. Kim, D. Kim, Y. Gogotsi, S. O. Kim and C. M. Koo, *Adv. Mater.*, 2020, **32**, 1906769.
10. C. J. Zhang, B. Anasori, A. Seral-Ascaso, S. H. Park, N. Mcevoy, A. Shmeliov, G. S. Duesberg, J. N. Coleman, Y. Gogotsi and V. Nicolosi, *Adv. Mater.*, 2017, **29**, 1702678.
11. T. Guo, D. Zhou, S. Deng, M. Jafarpour, J. Avaro, A. Neels, J. Heier and C. Zhang, *ACS Nano*, 2023, **17**, 3737-3749.
12. M. Mojtabavi, A. Vahidmohammadi, D. Hejazi, S. Kar, S. Shahbazmohamadi and M. Wanunu, *ACS Nano*, 2021, **15**, 625–636.
13. R. Li, X. Ma, J. Li, J. Cao and X. Ling, *Nat. Commun.*, 2021, **12**, 1587.
14. W. L. Song, X. T. Guan, L. Z. Fan, W. Q. Cao, C. Y. Wang, Q. L. Zhao and M. S. Cao, *J. Mater. Chem. A*, 2015, **3**, 2097-2107.
15. Q. Song, F. Ye, X. Yin, W. Li, H. Li, Y. Liu, K. Li, K. Xie, X. Li, Q. Fu, L. Cheng, L. Zhang and B. Wei, *Adv. Mater.*, 2017, **29**, 1701583.
16. L. Kong, X. Yin, M. Han, X. Yuan and J. Huang, *Carbon*, 2017, **111**, 94-102.
17. B. Shen, W. Zhai and W. Zheng, *Adv. Funct. Mater.*, 2014, **24**, 4542-4548.
18. L. Zhang, N. T. Alvarez, M. Zhang, M. Haase, R. Malik, D. Mast and V. Shanov, *Carbon*, 2015, **82**, 353-359.
19. K. Zou, J. Ge, L. Yan and N. Bao, *Ind. Eng. Chem. Res.*, 2022, **61**, 8782-8791.
20. S. Lin, H. Wang, F. Wu, Q. Wang, X. Bai, D. Zu, J. Song, D. Wang, Z. Liu and Z. Li, *npj Flex. Electron.*, 2019, **3**, 6.
21. J. Zhang, X. Li, M. Zhang, Q. Zhu and X. Sun, *Mater. Adv.*, 2022, **3**.
22. D. G. Kim, J. H. Choi, D.-K. Choi and S. W. Kim, *ACS Appl. Mater. Interfaces*, 2018, **10**, 29730-29740.
23. F. Shahzad, M. Alhabeb, C. B. Hatter, B. Anasori, S. Man Hong, C. M. Koo and Y. Gogotsi, *Science*, 2016, **353**, 1137-1140.

24. U. Ş. Yaşar and H. Kaya, *IEEJ Trans. Electr. Electron. Eng.*, 2024, **19**, 1756-1762.
25. Z. Chen, S. Yang, J. Huang, Y. Gu, W. Huang, S. Liu, Z. Lin, Z. Zeng, Y. Hu, Z. Chen, B. Yang and X. Gui, *Nano-Micro Lett.*, 2024, **16**, 92.
26. A. Ameli, M. Nofar, S. Wang and C. B. Park, *ACS Appl. Mater. Interfaces*, 2014, **6**, 11091–11100.
27. K. Ji, H. Zhao, J. Zhang, J. Chen and Z. Dai, *Appl. Surf. Sci.*, 2014, **311**, 351-356.
28. Z.-Y. Jiang, W. Huang, L.-S. Chen and Y.-H. Liu, *Opt. Express*, 2019, **27**, 24194-24206.
29. S. Shen, S.-Y. Chen, D.-Y. Zhang and Y.-H. Liu, *Opt. Express*, 2018, **26**, 27545-27554.
30. Z. Jiang, S. Zhao, L. Chen and Y.-h. Liu, *Opt. Express*, 2021, **29**, 18760-18768.
31. M. Han, X. Yin, K. Hantanasirisakul, X. Li, A. Iqbal, C. B. Hatter, B. Anasori, C. M. Koo, T. Torita and Y. Soda, *Adv. Opt. Mater.*, 2019, **7**, 1900267.
32. A. Iqbal, F. Shahzad, K. Hantanasirisakul, M. K. Kim, J. Kwon, J. Hong, H. Kim, D. Kim, Y. Gogotsi and C. M. Koo, *Science*, 2020, **369**, 446-450.
33. M. Han, C. E. Shuck, R. Rakhmanov, D. Parchment, B. Anasori, C. M. Koo, G. Friedman and Y. Gogotsi, *ACS Nano*, 2020, **14**, 5008-5016.
34. Z. Zhuang, H. Chen and C. Li, *ACS Nano*, 2023, **17**, 10628-10636.
35. W. Li, T. Zhou, Z. Zhang, L. Li, W. Lian, Y. Wang, J. Lu, J. Yan, H. Wang, L. Wei and Q. Cheng, *Science*, 2024, **385**, 62-68.
36. S. Wan, Y. Chen, C. Huang, Z. Huang, C. Liang, X. Deng and Q. Cheng, *Nature*, 2024, **634**, 1103–1110.
37. S. Wan, X. Li, Y. Chen, N. Liu, S. Wang, Y. Du, Z. Xu, X. Deng, S. Dou and L. Jiang, *Nat. Commun.*, 2022, **13**, 7340.
38. S. Wan, X. Li, Y. Chen, N. Liu, Y. Du, S. Dou, L. Jiang and Q. Cheng, *Science*, 2021, **374**, 96-99.
39. J. Zhang, N. Kong, S. Uzun, A. Levitt, S. Seyedin, P. A. Lynch, S. Qin, M. Han, W. Yang, J. Liu, X. Wang, Y. Gogotsi and J. M. Razal, *Adv. Mater.*, 2020, **32**, 2001093.
40. G. S. Lee, T. Yun, H. Kim, I. H. Kim, J. Choi, S. H. Lee, H. J. Lee, H. S. Hwang, J. G. Kim, D.-w. Kim, H. M. Lee, C. M. Koo and S. O. Kim, *ACS Nano*, 2020, **14**, 11722-11732.